Received: 11 December 2023 | Revised: 26 February 2024 | Accepted: 26 April 2024

DOI: 10.1111/vsu.14099

WILEY

CASE REPORT

Three-dimensionally printed osteotomy and reaming guides for correction of a multiplanar femoral deformity stabilized with an interlocking nail in a dog

Logan M. Scheuermann DVM, MS | **Stanley E. Kim BVSc, MS, DACVS (Small Animal)**

Department of Small Animal Clinical Sciences, College of Veterinary Medicine, University of Florida, Gaincesville, Florida, USA

Correspondence
Stanley E. Kim, Department of Small Animal Clinical Sciences, College of Veterinary Medicine, University of Florida, Gainesville, FL 32610, USA.
Email: stankim@ufl.edu

Abstract

Objective: To describe the use of virtual surgical planning (VSP) and three-dimensionally (3D) printed surgical guides for corrective osteotomies stabilized with an interlocking nail in a dog with a multiplanar femoral deformity.

Study design: Case report.

Animals: An 8-year-old male neutered mixed breed dog weighing 44 kg.

Methods: A dog was presented for a right grade 3 lateral patellar luxation secondary to a multiplanar femoral deformity due to a suspected femoral malunion. A computed tomography (CT) scan was obtained to create virtual femoral models. Corrective osteotomies were simulated with VSP. Custom osteotomy guides and reaming guides were designed to facilitate the correction and the placement of an interlocking nail. The preoperative femoral model, virtually aligned femoral model, custom osteotomy guides, and reaming guides were 3D printed, sterilized, and utilized intraoperatively. A CT scan was performed postoperatively to assess femoral length and alignment.

Results: Custom osteotomy and reaming guides were used as intended by the VSP. Postoperative femoral length as well as frontal, sagittal, and axial plane alignment were within 0.7 mm, 2.2°, 0.5°, and 1.6°, respectively, of the virtually planned femoral model. Two months postoperatively, the dog was sound on visual gait examination, and the patella tracked in the trochlear groove throughout stifle range of motion and was unable to be manually luxated. Radiographs obtained 2 months postoperatively revealed static femoral alignment and implants. Both osteotomies were discernable with callus bridging.

Conclusion: Virtual surgical planning and custom osteotomy and reaming guides facilitated complex femoral corrective osteotomies and interlocking nail placement.

1 | INTRODUCTION

Lateral patellar luxation is associated with congenital, developmental, or traumatic abnormalities of the pelvic limb, causing impaired quadriceps function and potential lameness.[1,2] Higher grades of patellar luxation are frequently associated with femoral deformities, which are more likely to require corrective osteotomies to reduce the risk of reluxation postoperatively compared to trochleoplasty and tibial tuberosity transposition.[1,3,4] Assessment of femoral deformities when using radiographs can be challenging, especially for multiplanar

deformities with torsional abnormalities.[4–6] As such, computed tomography (CT) is often the preferred imaging modality as it allows for more accurate quantification of alignment in three dimensions than radiographs.[7,8]

Distal femoral osteotomy is an effective treatment for patellar luxation and concurrent femoral deformity, particularly for frontal plane malalignment.[3,4] Virtual surgical planning (VSP) and three-dimensional (3D) printing of custom surgical guides have recently been utilized for distal femoral osteotomies in dogs.[9] In a study by Hall and colleagues, 3D-printed distal femoral osteotomy and reduction guides facilitated correction of distal femoral varus and femoral torsion within 2.3° and 1.7°, respectively, of the preoperative virtual plan.[9]

Deformity corrections with interlocking nails may be advantageous as they are biomechanically robust and theoretically facilitate axial alignment.[10–13] Correction of distal femoral deformities with an interlocking nail has been previously described[10,14,15] but the procedure may be technically difficult, particularly with complex deformities. During interlocking nail placement, accurate bolt placement can be challenging, especially for distal bolts.[10,16] Although 3D-printed guides can generate accurate distal femoral osteotomies that are stabilized with bone plates, conventional guide designs may not be suitable for use with interlocking nails.

The objective of this case report is to describe the successful correction of a biapical multiplanar femoral malunion in a dog, utilizing VSP and 3D-printing of custom osteotomy, drilling, and reaming guides for placement of an interlocking nail.

2 | MATERIALS AND METHODS

An 8-year-old male neutered mixed-breed dog was presented for evaluation of a right pelvic limb lameness. The dog reportedly had a pelvic limb lameness since the time of adoption, 4 years before presentation. Six months prior to presentation at the authors' institution, the dog was presented to its primary veterinarian for evaluation of the lameness and was diagnosed with right lateral patellar luxation. On presentation at the authors' institution, orthopedic examination revealed a grade 2 right pelvic limb lameness with a right grade 3 lateral patellar luxation.[17] The dog weighed 45.6 kg and was obese with a body condition score of 9/9. Bilateral orthogonal femoral radiographs were obtained and revealed a biapical, femoral valgus deformity with recurvatum and internal torsion secondary to a suspected femoral malunion (Figure 1A,B). There was right tarsal hyperextension during standing and ambulation. A CT scan (Aquilion Prime S computed tomography scanner, Canon Medical Systems USA, Tustin, California) of both pelvic limbs was obtained for surgical planning using a slice thickness of 0.5 and 0.3 mm slice overlap.

Utilizing the bone algorithm volumetric CT data, Digital Imaging and Communications in Medicine (DICOM) files were imported into an image processing software program (Mimics, Materialize NV, Leuven, Belgium) and segmented. Virtual bone models of the affected and contralateral femur were created and imported into a biomodelling software program (3-matic, Materialize NV). The proximal and distal centers of rotation of angulation

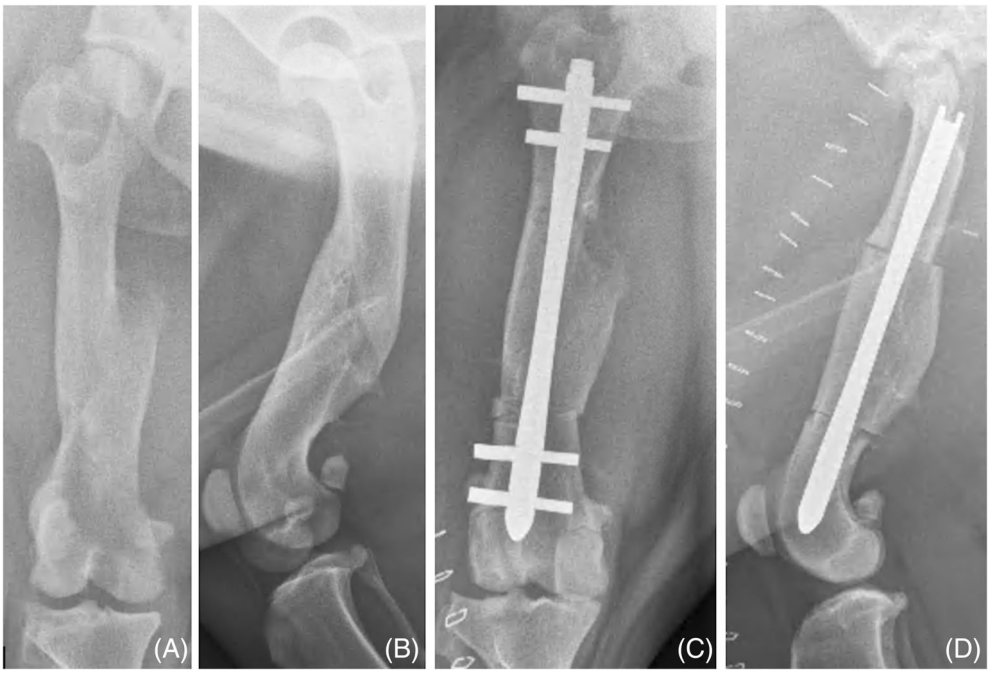

FIGURE 1 Preoperative (A) craniocaudal and (B) lateromedial radiographs of the right femur and immediate postoperative (C) craniocaudal and (D) lateromedial radiographs of the aligned right femur stabilized with an I-Loc nail.

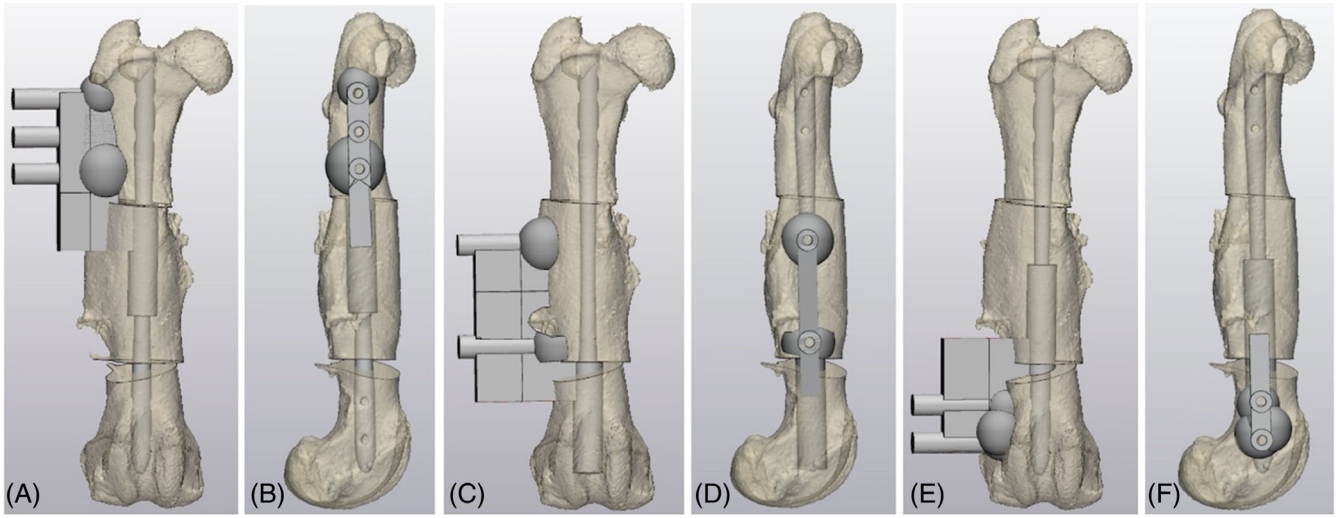

FIGURE 2 Cranial (A, C, E) and lateral (B, D, F) views of the virtually aligned femoral model with a virtually placed I-Loc nail and a proximal (A, B), middle (C, D), or distal reaming guide (E, F).

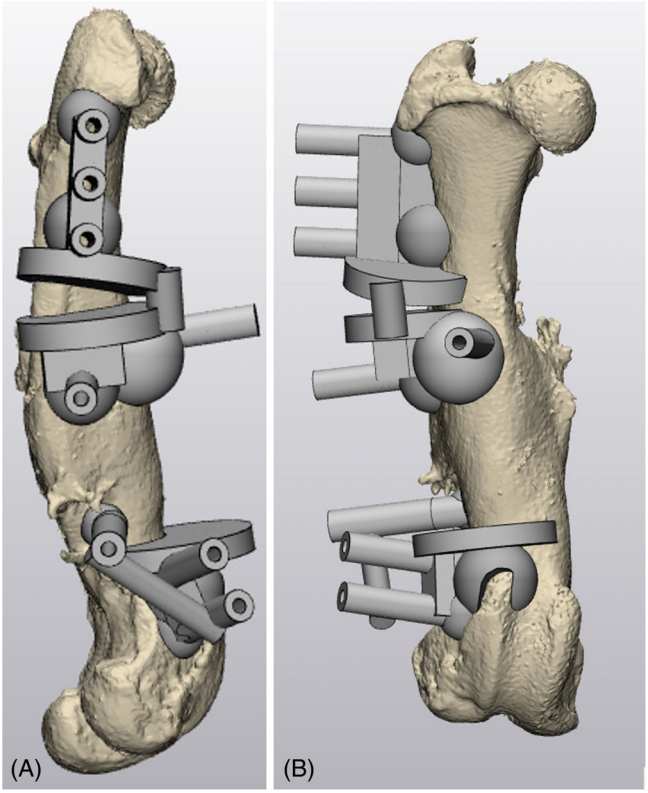

FIGURE 3 Lateral (A) and cranial (B) view of the preoperative virtual femoral model and custom osteotomy guides applied.

(CORA) were identified on the affected femur and the magnitude of angulation at each CORA was measured in the frontal and sagittal plane using the anatomic axis of each femoral segment.[18] Torsional alignment of each segment was determined by measuring the angulation in the axial plane between the linea aspera of each femoral segment. At the proximal CORA, there was 14.8° of varus, 10.3° of recurvatum, and 15.0° of external torsion. At the distal CORA there was 20.5° of valgus and 62.9° of procurvatum, and 50.0° of internal torsion. A simulated laterally based proximal closing wedge ostectomy was created at the level of the proximal CORA. A virtual 3D mirror image of the contralateral femur and the affect femur were overlaid, aligning the proximal segments of each femur. The middle femoral segment was reduced until its anatomic axis was parallel to the equivalent

anatomic axis of the mirror image of the contralateral femur and it was well aligned with the proximal segment in the frontal, sagittal, and axial planes. Then a laterally based distal opening wedge osteotomy was created at the level of the distal CORA. The distal femoral segment was realigned until its anatomic axis was parallel to the equivalent anatomic axis of the mirror image of the contralateral femur in the frontal and axial planes and the distal femoral procurvatum was reduced to facilitate interlocking nail placement. The reduced proximal, middle, and distal femoral segments were combined using Boolean union.

A CT scan of a 135 mm long, 8 mm diameter interlocking nail (I-Loc IM Fixator Biomedtrix, Movora, Whippany, New Jersey) was acquired using the same technique as the pelvic limbs. Single energy metal artifact reduction (Canon Medical Systems USA) was used to reduce the metal artifact.[19–21] The DICOM files were segmented to create a virtual interlocking nail, which was imported into the planning software and placed within the medullary canal of the realigned virtual femoral model. Based on the virtually aligned femoral model, custom proximal, middle, and distal reaming guides were designed to facilitate placement of the nail and associated bolts in the planned nail location to theoretically align the femoral segments. The custom reaming guides consisted of lateral pin sleeves, a custom base that conformed to the lateral femoral topography, as well as a cannulated reaming sleeve contoured to the osteotomized surface of the femoral segment (Figure 2). The base was designed with a clearance of 0.3 mm to account for periosteum and regional soft tissues that were not present on the bone models. The pin sleeves of the proximal and distal reaming guides were placed at the planned level of the four nail cannulations and were designed to accommodate 3.2 mm half pins. The proximal reaming guide also contained an additional pin sleeve distal to the nail cannulations. The middle reaming guide had a pin sleeve at the proximal and distal aspect of the middle femoral segment and the reaming sleeve conformed to the distal osteotomy surface.

Custom proximal and distal osteotomy guides were designed to conform to the femoral topography at the level of each CORA (Figure 3). Both osteotomy guides consisted of pin sleeves to accommodate 3.2 mm half pins; osteotomy shelves; and custom bases, with a clearance of 0.3 mm, which connected the pin sleeves and osteotomy shelves. The osteotomy guides were initially designed based on the virtually aligned femur with the lateral pin sleeves corresponding to the reaming guide pin sleeves. The middle and distal femoral segments and associated lateral pin sleeves were translated and superimposed over the intact, affected virtual femoral model. The proximal ostectomy guide consisted of the three pin sleeves corresponding to the proximal reaming guide pin sleeves, a distal pin sleeve corresponding to the proximal pin sleeve of the middle reaming guide, a cranial pin sleeve, and two laterally based osteotomy shelves, each with a 16 mm radius, to generate a laterally based proximal closing wedge ostectomy. The distal osteotomy guide consisted of the two pin sleeves corresponding to the distal reaming guide pin sleeves and nail cannulations, a proximal pin sleeve corresponding to the distal pin sleeve of the middle reaming guide, and a single osteotomy shelf, with a 17 mm radius, to generate a laterally based distal opening wedge osteotomy (Figure 3).

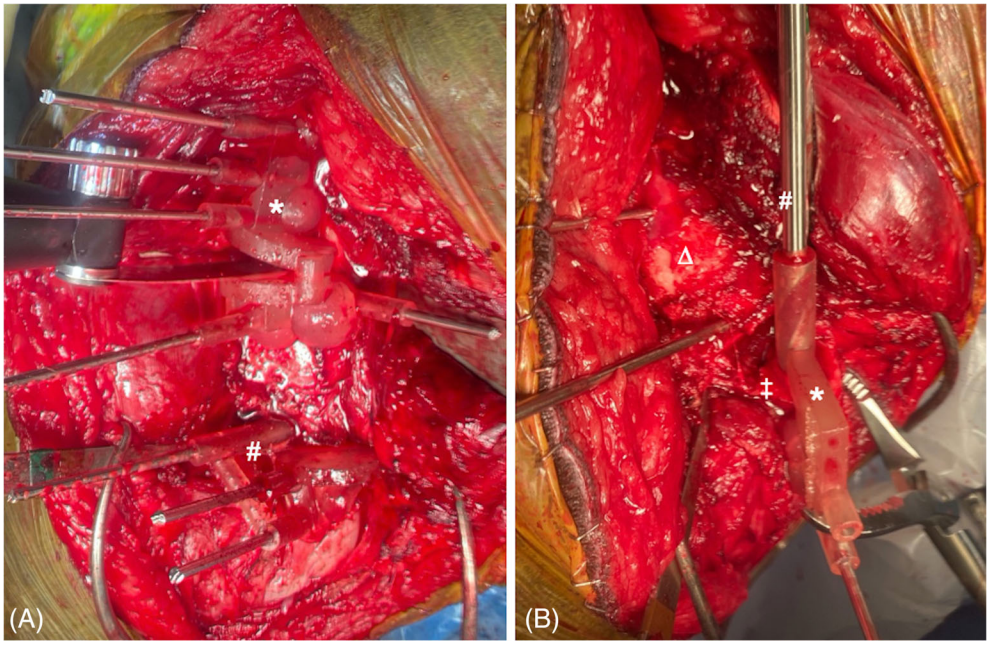

FIGURE 4 Intraoperative images of 3D-printed surgical guides: (A) Craniolateral image of the applied proximal (*) and distal (#) osteotomy guides. (B) Distal reaming guide (*), a 4.5 mm drill bit (#) reaming the distal femoral segment (‡) retrograde, and the middle femoral segment (Δ).

The affected preoperative and aligned femoral models as well as the custom osteotomy and reaming guides were 3D-printed in a biocompatible resin (BioMed Amber Resin, Formlabs, Sommerville, Massachusetts) using a stereolithography 3D printer (Form 3BL, Formlabs). The 3D-printed bone models and custom surgical guides were processed and cured according to the manufacturer's guidelines and steam sterilized.[22]

Surgery was performed 72 days after the initial evaluation. The dog was anesthetized and right preiliac femoral and parasacral sciatic nerve blocks were performed using dexmedetomidine 0.22 μg/kg and bupivacaine 0.33 mg/kg. Cefazolin (22 mg/kg IV) was administered after induction of anesthesia and every 90 min intraoperatively. With the dog in dorsolateral oblique recumbency, a lateral approach to the right femur and a lateral parapatellar approach to the right stifle were performed. Osteotomy guides were applied to their positions of optimal fit and affixed with "1/8" Steinmann pins (Figure 4A). The proximal and distal osteotomies were performed and osteotomy guides were removed, without removing the Steinmann pins. The proximal, middle, and distal reaming guides were applied over the Steinmann pins and the medullary canal was reamed retrograde with a 4.5 mm drill bit (Figure 4B). While reaming, Steinmann pins were removed sequentially to facilitate reaming of the medullary cavity. The reaming guides were removed. The awl was then used to further prepare the medullary cavity of each segment and a 135 mm 8 mm interlocking nail was inserted in normograde fashion into the proximal and middle segments then driven into the and distal femoral segment. Osteotomy reduction was assessed intraoperatively using fluoroscopy. Rotational and proximodistal alignment of the nail cannulations and bone tunnels created by the surgical guides was assessed visually using the I-Loc insertion handle and the alignment guide (Biomedtrix, Movora), respectively. A needle arthroscope (Nanoscope, Arthrex Vet Systems, Naples, Florida) was inserted through the cis femoral cortex of the tracts created by the previous Steinmann pins to ensure appropriate nail positioning before bolt insertion. The cis and trans cortices of the pin tracts were overdrilled using 4.3 and 3.2 mm drill bits, respectively, and four locking bolts were inserted. The ostectomized corticocancellous wedge from the proximal ostectomy was inserted in the distal opening wedge osteotomy. Postoperative right femoral radiographs were made to confirm appropriate implant positioning and femoral alignment.

Postoperatively, the dog was managed with cefazolin (22 mg/kg IV) every 8 h for 24 h and transitioned to cephalexin (22 mg/kg orally) every 12 h, carprofen (2.2 mg/kg orally) every 12 h, a fentanyl constant rate infusion (2–3 μg/kg/h IV) for 18 h, and gabapentin (13 mg/kg orally) every 8 h. The dog was discharged 2 days postoperatively.

Evaluations at 1 and 3 weeks postoperatively included orthopedic examinations. A 2-month postoperative evaluation consisted of an orthopedic examination and orthogonal right femoral radiographs in addition to a CT scan of the pelvic limbs using the same technique as the preoperative CT scan. Single energy metal artifact reduction (Canon Medical Systems USA) was used. A 10-month postoperative evaluation consisted of an orthopedic examination and orthogonal right femoral and tarsal radiographs. Computed tomography DICOM files were exported to a modeling software program (Mimics, Materialize NV) for segmentation and creation of 3D virtual bone models. Virtual femoral models were imported into 3-matic (Materialize NV). Femoral length, frontal plane alignment,[23] sagittal plane alignment,[24] and femoral torsion[25] were measured for the

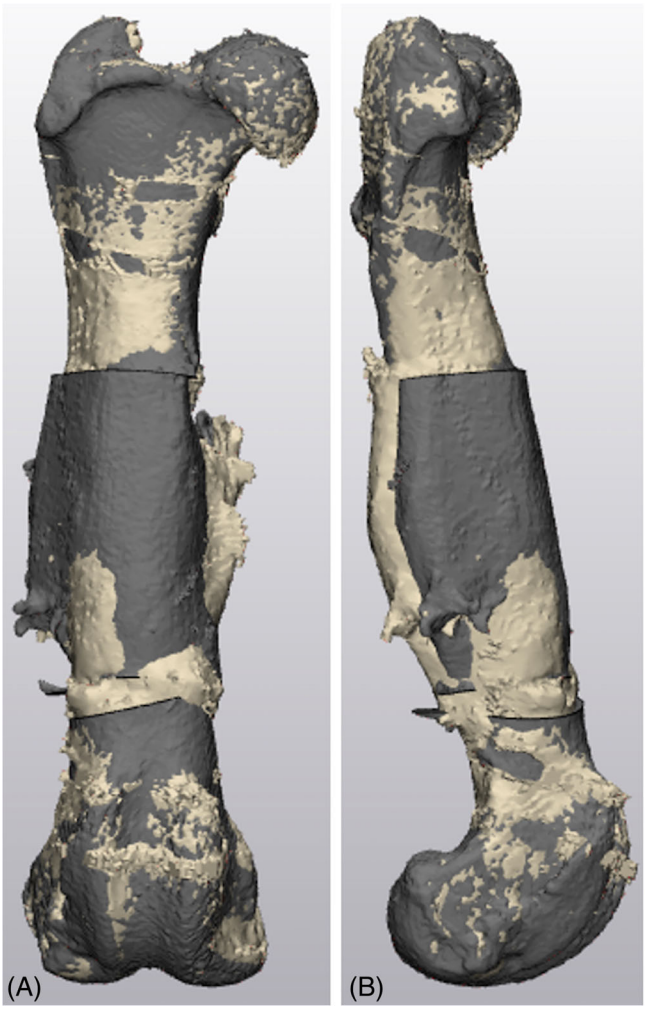

FIGURE 5 (A) Cranial view of the virtually planned femoral alignment (gray) and postoperative femora (tan) superimposed. (B) Lateral view of the virtually planned femoral alignment (gray) and postoperative femora (tan) superimposed.

contralateral, preoperative, virtually aligned, and the 2 month postoperative femora.[26]

3 | RESULTS

The custom osteotomy and reaming guides were used intraoperatively without any deviation from the intended VSP (Figure 1C,D). Total surgical duration was 149 min. One day postoperatively, the dog was non-weight-bearing lame in the right pelvic limb with mild soft-tissue swelling of the right thigh. The right patella tracked in the trochlear groove throughout stifle range of motion and could not be manually luxated. At 1 and 3 weeks postoperatively, the dog was intermittently non-weight-bearing lame in the right pelvic limb. Throughout the stifle range of motion at the 1- and 3-week re-evaluations, the patella tracked in the trochlear groove and was unable to be manually luxated.

Postoperative femoral length was 0.7 mm shorter than the virtual plan (Figure 5) and 1.2 mm longer than the preoperative femur. The postoperative femoral length was 20.4% shorter than the contralateral femur (Table 1). The corrected femur had a 17.7° increase in femoral varus compared to the preoperative frontal plane alignment. Compared to the contralateral and virtually planned femoral varus, the postoperative femur had 3.8° and 2.2° increased femoral varus, respectively. Sagittal plane alignment postoperatively was within 0.4° of the virtual plan with an increase in recurvatum. The corrected femur had 17.5° less recurvatum than the preoperative femur and 11.4° more recurvatum than the contralateral femur. Femoral torsion of the postoperative femur was 1.6° and 2.8° greater (i.e., more anteversion) than the virtually planned femur and contralateral femur, respectively, and 17.2° less (i.e., more normoverted) than the preoperative femur.

Two months postoperatively, the dog was sound on visual gait exam and the patella tracked in the trochlear groove throughout stifle range of motion could not be manually luxated. Orthogonal radiographs (Figure 6A,B) and a CT scan (Figure 7) 2 months postoperatively revealed static femoral alignment and implants. Both

TABLE 1 Contralateral, preoperative, virtually planned, and postoperative femoral length, and alignment.

	Femoral length (mm)	Frontal plane mLDFA (°)	Sagittal plane mCdDFA (°)	Axial plane Torsion (°)
Contralateral femur	189.4	95.1	25.2	34.5
Preoperative femur	149.5	81.2	54.1	54.5
Virtually planned femur	151.4	96.7	37.0	35.7
Postoperative femur	150.7	98.9	36.6	37.3

Abbreviations: mCdDFA, mechanical caudal distal femoral angle; mLDFA, mechanical lateral distal femoral angle; mLPFA, mechanical lateral proximal femoral angle.

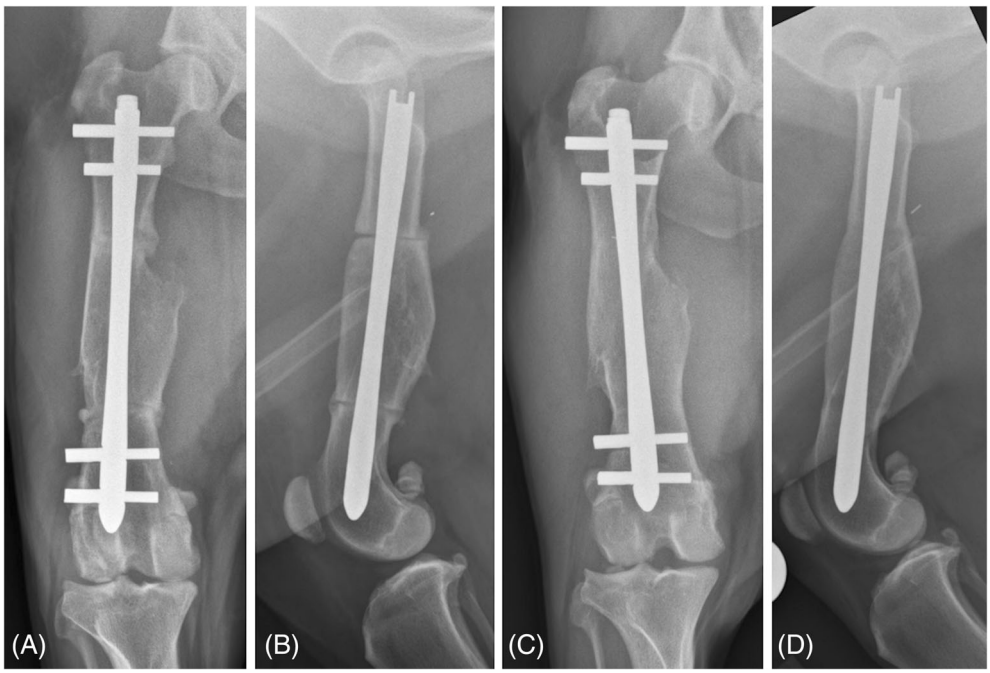

FIGURE 6 Two-month postoperative craniocaudal (A) and lateromedial (B) radiographs of the right femur and 10 month postoperative craniocaudal (C) and lateromedial (D) radiographs of the right femur.

FIGURE 7 Virtual three-dimensional reconstruction of the computed tomography scan 2 month postoperatively. Craniocaudal (A) and lateromedial (B) view of the right femur 2 months postoperative.

osteotomies were discernable with callus bridging. The dog was re-evaluated 10 months postoperatively. On orthopedic examination, the dog had tarsal hyperextension, which was comparable to findings from the preoperative examination. The patella tracked normally in the trochlear groove without luxation. Orthogonal right femoral radiographs revealed union of the osteotomies with homogenous femoral cortices and no visible osteotomy lines (Figure 6C,D). The interlocking nail and bolts were stable without peri-implant lucency. Orthogonal tarsal radiographs were unremarkable.

4 | DISCUSSION

Virtual surgical planning and 3D-printed custom osteotomy and reaming guides were used to facilitate accurate interlocking nail placement and correction of a complex femoral deformity in a dog. Correction was deemed highly accurate, with postoperative femoral length and frontal, sagittal, and axial plane alignment within 0.7 mm, 2.2°, 0.5°, and 1.6°, respectively, of the virtually planned femoral model. This level of accuracy could have been more challenging to achieve using traditional preoperative planning and intraoperative techniques.

The outcome of this case is consistent with the findings from previous reports on the use of custom 3D-printed guides for deformity correction in dogs. In a prospective study, Hall and colleagues reported accurate distal femoral ostectomy stabilized with locking plates in 10 dogs with medial patellar luxation utilizing custom osteotomy and reduction guides.[9] Hall et al. reported similar postoperative discrepancies in mean distal femoral varus and femoral torsion of 2.3° and 1.7°, respectively, compared with the target femoral alignment.[9] De Armond and colleagues also reported accurate deformity correction utilizing custom surgical guides for antebrachial deformities with mean radial frontal, sagittal, and axial angulation within 1.8°, 2.5°, and 3.5°, respectively, of the virtually planned alignment.[27]

In the current study, the contralateral femur was used to assist with preoperative planning, but a perfect replication of normal femoral morphology was not the aim. Compared to the contralateral femur postoperative femoral varus and torsion were accurately corrected with 3.8° increased varus and 2.8° anteversion. The affected femur, however, had 11.4° more recurvatum postoperatively, which was attributed to intentional overreduction in the sagittal plane to facilitate interlocking nail placement. Sagittal plane malalignment tends to be better tolerated than malalignment in other planes;[18] however, the overreduction of the distal femoral segment in the sagittal plane associated with use of a straight interlocking nail may contribute to extensor mechanism malalignment.[28] Femoral shortening was not addressed, as femoral lengthening is technically difficult and associated with a high complication rate.[29] Alternatively, acute femoral length correction could have been performed by utilizing opening wedge osteotomies both proximally and distally. The proximal closing wedge ostectomy performed in the present case may decrease the total bone length but straightening of the femur may result in increased functional femoral length and increased tension on the quadriceps muscles.[30] Similarly, as shortening the femur during femoral ostectomies improves stifle range of motion and may reduce the risk of patellar luxation,[31] increasing femoral length and the resultant tension of the quadriceps and hamstring muscle groups might impair stifle range of motion postoperatively and increase the risk

of patellar luxation. Due to the soft tissue constraints of the quadriceps muscles, we often shorten the femur by 5 mm to 1 cm during distal femoral ostectomies. Femoral length was 20.4% shorter in the affected, postoperative femur than the contralateral femur. Franczuszki and colleagues demonstrated that dogs can tolerate an acute 20% femoral shortening and maintain full weight bearing by increasing the standing angle of the affected limb joints and decreasing the flexion angles of joints on the contralateral limb.[32] The dog in the present report had a 20% femoral length discrepancy preoperatively and postoperatively and within 2 months postoperatively, was sound on visual gait examination. Consistent with Franczuszki and colleagues' report, the dog exhibited tarsal hyperextension postoperatively, likely due to the length discrepancy between the pelvic limbs. An acute femoral length correction may have likely reduced the degree of postoperative tarsal hyperextension.

Stabilization of femoral deformity corrections with interlocking nails has been described previously.[10,14,15] An interlocking nail was selected in the present case for multiple reasons. Interlocking nail placement within the medullary canal facilitates frontal plane realignment. Femoral osteotomies are commonly stabilized utilizing plates with infrequent implant failure,[3,4,30] but interlocking nails are biomechanically favorable to placement of eccentrically placed plates as interlocking nails are placed closer to the neutral axis of the femur, minimizing bending moments during weight bearing. The location of proximal and distal bolts in the femoral metaphysis allowed for a single implant to bridge multiple osteotomies, whereas multiple implant constructs may have been required with plate fixation. Finally, distal femoral plates must be placed in close proximity to, or over, the stifle joint capsule, which may lead to local irritation.[3,30]

An 8 mm nail was selected based on the dog's body weight and femoral medullary canal diameter. The use of a 7 mm nail, however, would have increased construct compliance and might have reduced the time to union of the osteotomies. Fatigue failure of an angle-stable interlocking nail is rare and may have been unlikely with the 7 mm nail due to the load sharing with the cortices but an 8 mm nail was selected for the present case to reduce the risk of bolt fatigue failure.[10] In the authors' clinical experience, the most common mode of failure with interlocking nails is not fatigue failure of the nail but of the proximal bolts. Use of an 8 mm nail increased the canal fill, thus increasing the fatigue life of the bolts.[33] We considered the larger core diameters (and corresponding higher area moment of inertia) of the interlocking bolts used with the 8 mm nail (cis-cortex: 4.3 mm, trans-cortex: 3.2 mm) compared with the 7 mm nail (cis-cortex: 3.5 mm, trans-cortex: 2.7 mm) to be clinically significant.

The custom surgical guides featured multiple novel components. Appropriate segment alignment relied on accurate positioning of the interlocking nail, and intramedullary reaming guides were therefore designed that created a suitable path for the nail in all three major segments. These reaming guides were affixed with the same half pins used to secure the osteotomy guides; these pins intruded into the medullary canal, although this limitation was overcome easily by sequentially and partially removing the half pins as the reamer was advanced. Another novel feature was the positioning of half pins in the proximal and distal femoral segments as they were placed at the planned location of the interlocking bolts. Accurate placement of bolts is a critical step in interlocking nail placement and can be particularly challenging for distal bolts.[10,16,34] The predrilled bolt holes were well aligned to the interlocking nail as it was accurately positioned in the reamed intramedullary canal. In the present case, verification of accurately drilled tracts for bolt placement was confirmed by placing a needle arthroscope through the cis cortical tract after interlocking nail placement to visualize the threaded nail cannulations.

There are multiple potential limitations of the described application of virtual surgical planning and 3D-printed custom surgical guides for femoral deformity correction and interlocking nail placement. The custom surgical guides in the present case facilitated accurate correction of femoral alignment but the use of reaming guides for interlocking nail placement may increase the number of guides required to be designed, printed, and applied intraoperatively compared with osteotomy stabilization with plates. A custom reaming guide is required for each bone segment to facilitate accurate nail placement, whereas a single reduction guide can be transiently used to stabilize an osteotomy during plate application.[9] Accurate postoperative alignment, utilizing the described custom osteotomy and reaming guides, relies on accurate nail and bolt placement. Placement of the bolts is determined by the placement of the osteotomy guides; however, when utilizing 3D-printed custom surgical guides minor discrepancies are expected in intraoperative guide placement and the associated bone alignment when compared with the virtual plan.[9,27,35] To verify accurate nail and bolt placement, fluoroscopy and a needle arthroscope were used intraoperatively, as in the authors' experience, sensation from the feeler wire can be misleading because trabecular bone can mimic the nail threads. The use of fluoroscopy and a needle arthroscopy may be unnecessary, however, if guide placement is accurate and the feeler wire is used to identify the threaded nail cannulations. Bolt

placement was accurate in the present case but if the nail cannulations are unable to be identified through the predrilled cis cortical tracts, fluoroscopy may be used to assess nail placement and the location of the cortical tract. Inaccurate bolt or nail placement when utilizing the present system may require the redrilling of bolt holes based on the expected nail location within the medullary canal based on preoperative planning, use of the alignment guide, or intraoperative fluoroscopy (i.e., removing the guide system) and additional reaming of the medullary canal. The periosteal blood supply in the present case may have been affected in a similar manner to cases in which femoral osteotomies are stabilized using one or more plates due to the dissection required for patient-specific guide application.

Utilization of virtual surgical planning and 3D-printing custom osteotomy and reaming guides facilitated accurate femoral deformity correction and interlocking nail placement. Both ex vivo and clinical studies may be helpful to further evaluate the accuracy of custom reaming guides for interlocking nail placement during correction of angular limb deformities.

AUTHOR CONTRIBUTIONS

Scheuermann LM, DVM, MS: Conceptualization and contribution to the design of the surgical plan, data collection and interpretation, manuscript preparation and revision. Kim SE, BVSc, MS, DACVS (Small Animal): Conceptualization and contribution to the design of the surgical plan, data collection and interpretation, manuscript preparation and revision. Both authors approved the final version of the submitted article.

CONFLICT OF INTEREST

The authors declare no conflicts of interest related to this report.

REFERENCES

1. Perry KL, Déjardin LM. Canine medial patellar luxation. *J Small Anim Pract*. 2021;62(5):315-335.
2. Roy RG, Wallace LJ, Johnston GR, Wickstrom SL. A retrospective evaluation of stifle osteoarthritis in dogs with bilateral medial patellar luxation and unilateral surgical repair. *Vet Surg*. 1992;21(6):475-479.
3. Brower BE, Kowaleski MP, Peruski AM, et al. Distal femoral lateral closing wedge osteotomy as a component of comprehensive treatment of medial patellar luxation and distal femoral varus in dogs. *Vet Comp Orthop Traumatol*. 2017;30(1):20-27.
4. Swiderski JK, Palmer RH. Long-term outcome of distal femoral osteotomy for treatment of combined distal femoral varus and medial patellar luxation: 12 cases (1999–2004). *J Am Vet Med Assoc*. 2007;231(7):1-6.
5. Jackson GM, Wendelburg KL. Evaluation of the effect of distal femoral elevation on radiographic measurement of the anatomic lateral distal femoral angle. *Vet Surg*. 2012;41(8):994-1001.
6. Adams RW, Gilleland B, Monibi F, Franklin SP. The effect of valgus and varus femoral osteotomies on measures of anteversion in the dog. *Vet Comp Orthop Traumatol*. 2017;30(3):184-190.
7. Dudley RM, Kowaleski MP, Drost WT, Dyce J. Radiographic and computed tomographic determination of femoral varus and torsion in the dog. *Vet Radiol Ultrasound*. 2006;47(6):546-552.
8. Yasukawa S, Edamura K, Tanegashima K, et al. Evaluation of bone deformities of the femur, tibia, and patella in toy poodles with medial patellar luxation using computed tomography. *Vet Comp Orthop Traumatol*. 2016;29(1):29-38.
9. Hall EL, Baines S, Bilmont A, Oxley B. Accuracy of patient-specific three-dimensional-printed osteotomy and reduction guides for distal femoral osteotomy in dogs with medial patella luxation. *Vet Surg*. 2019;48(4):584-591.
10. Déjardin LM, Perry KL, von Pfeil DJF, Guiot LP. Interlocking nails and minimally invasive osteosynthesis. *Vet Clin North Am Small Anim Pract*. 2020;50(1):67-100.
11. Déjardin LM, Lansdowne JL, Sinnott MT, Sidebotham CG, Haut RC. In vitro mechanical evaluation of torsional loading in simulated canine tibiae for a novel hourglass-shaped interlocking nail with a self-tapping tapered locking design. *Am J Vet Res*. 2006;67(4):678-685.
12. Lansdowne JL, Sinnott MT, Déjardin LM, Ting D, Haut RC. In vitro mechanical comparison of screwed, bolted, and novel interlocking nail systems to buttress plate fixation in torsion and mediolateral bending. *Vet Surg*. 2007;36(4):368-377.
13. Déjardin LM, Guillou RP, Ting D, Sinnott MT, Meyer E, Haut RC. Effect of bending direction on the mechanical behaviour of interlocking nail systems. *Vet Comp Orthop Traumatol*. 2009;22(4):264-269.
14. Witte PG, Scott HW. Treatment of lateral patellar luxation in a dog by femoral opening wedge osteotomy using an interlocking nail. *Vet Rec*. 2011;168(9):243.
15. Guillou RP, Guiot LP, Déjardin LM. Angle-stable interlocking nail fixation for distal femoral corrective osteotomy associated with medial patellar luxation. *Vet Comp Orthop Traumatol*. 2013;26(4):A11.
16. Duhautois B. Use of veterinary interlocking nails for diaphyseal fractures in dogs and cats: 121 cases. *Vet Surg*. 2003;32(1):8-20.
17. Quinn MM, Keuler NS, Lu Y, Faria MLE, Muir P, Markel MD. Evaluation of agreement between numerical rating scales, visual analogue scoring scales, and force plate gait analysis in dogs. *Vet Surg*. 2007;36(4):360-367.
18. Paley D, Herzenberg JE, Tetsworth K, McKie J, Bhave A. Deformity planning for frontal and sagittal plane corrective osteotomies. *Orthop Clin North Am*. 1994;25(3):425-465.
19. Wei F, Li J, Zhou C, et al. Combined application of single-energy metal artifact reduction and reconstruction techniques in patients with cochlear implants. *J Otolaryngol Head Neck Surg*. 2020;49(1):1-9.
20. Yasaka K, Kamiya K, Irie R, Maeda E, Sato J, Ohtomo K. Metal artefact reduction for patients with metallic dental fillings in helical neck computed tomography: comparison of adaptive iterative dose reduction 3D (AIDR 3D), forward-projected model-based iterative reconstruction solution (FIRST) and AIDR 3D with single-energy metal artefact reduction (SEMAR). *Dentomaxillofacial Radiol*. 2016;45(7):1-7.

21. Kawahara D, Ozawa S, Yokomachi K, et al. Metal artifact reduction techniques for single energy CT and dual-energy CT with various metal materials. *BJR Open*. 2019;1(1):1-7.
22. Formlabs. *Form Cure Manual*. 2019. Accessed July 9, 2021 https://media.formlabs.com/m/239b1aa5006cf5ff/original/-ENUS-Form-Cure-Manual.pdf
23. Tomlinson J, Fox D, Cook JL, Keller GG. Measurement of femoral angles in four dog breeds. *Vet Surg*. 2007;36(6):593-598.
24. Peterson JL, Torres BT, Hutcheson KD, Fox DB. Radiographic determination of normal canine femoral alignment in the sagittal plane: a cadaveric pilot study. *Vet Surg*. 2020;49(6):1230-1238.
25. Serck BM, Karlin WM, Kowaleski MP. Comparison of canine femoral torsion measurements using the axial and biplanar methods on three-dimensional volumetric reconstructions of computed tomography images. *Vet Surg*. 2021;50(7):1518-1524.
26. Scheuermann LM, Kim SE, Lewis DD, Johnson MD, Biedrzycki AH. Minimally invasive plate osteosynthesis of femoral fractures with 3D-printed bone models and custom surgical guides: a cadaveric study in dogs. *Vet Surg*. 2023;52(6):827-835.
27. De Armond CC, Lewis DD, Kim SE, Biedrzycki AH. Accuracy of virtual surgical planning and custom three-dimensionally printed osteotomy and reduction guides for acute uni- and biapical correction of antebrachial deformities in dogs. *J Am Vet Med Assoc*. 2022;1-9:1-9.
28. Silveira F, Monotti IC, Cronin AM, et al. Outcome following surgical stabilization of distal diaphyseal and supracondylar femoral fractures in dogs. *Can Vet J*. 2020;61(10):1073-1079.
29. Coutin JV, Lewis DD, Kim SE, Reese DJ. Bifocal femoral deformity correction and lengthening using a circular fixator construct in a dog. *J Am Anim Hosp Assoc*. 2013;49(3):216-223.
30. Kim SE, Lewis DD. Corrective osteotomy for procurvatum deformity caused by distal femoral physeal fracture malunion stabilised with string-of-pearls locking plates: results in two dogs and a review of the literature. *Aust Vet J*. 2014;92(3):75-80.
31. Nagahiro Y, Murakami S, Kamijo K, et al. Segmental femoral Ostectomy for the reconstruction of Femoropatellar joint in dogs with grade IV medial patellar luxation. *Vet Comp Orthop Traumatol*. 2020;33(4):287-293.
32. Franczuski D, Chalman J, Butler H, DeBowes R, Leipold H. Postoperative effects of experimental femoral shortening in the mature dog. *J Am Anim Hosp Assoc*. 1987;23:429-437.
33. Aper RL, Litsky AS, Roe SC, Johnson KA. Effect of bone diameter and eccentric loading on fatigue life of cortical screws used with interlocking nails. *Am J Vet Res*. 2003;64(5):569-573. doi: 10.2460/ajvr.2003.64.569
34. Durall I, Diaz MC, Morales I. Interlocking nail stabilization of humeral fractures: initial experiences in seven clinical cases. *Vet Comp Orthop Traumatol*. 1994;7(1):3-8.
35. Johnson MD, Lewis DD, Sutton WA, et al. Efficacy of two reduction methods in conjunction with 3-D–printed patient-specific pin guides for aligning simulated comminuted tibial fractures in cadaveric dogs. *Am J Vet Res*. 2022;83(9):1-10.

How to cite this article: Scheuermann LM, Kim SE. Three-dimensionally printed osteotomy and reaming guides for correction of a multiplanar femoral deformity stabilized with an interlocking nail in a dog. *Veterinary Surgery*. 2024;53(8):1438-1447. doi:10.1111/vsu.14099